
UFO: A Unified Flow-Oriented Framework for Robust Continual Graph Learning

Danhui Zhang¹, Zhe Wang¹, Qing Qing¹, Jiarui Liu¹, Wentao Gao², Ziqi Xu³,
Mingliang Hou⁴, Xikun Zhang³, Renqiang Luo¹

¹Jilin University, ²Adelaide University, ³RMIT University, ⁴Jinan University

Abstract

Graph learning research has increasingly shifted toward continual graph learning (CGL), which better reflects real-world scenarios where graphs evolve over time. However, existing CGL methods largely assume clean supervision and overlook a critical challenge: the newly arriving portions of the graph are often noisy, due to annotation errors or adversarial corruption. This mismatch limits their applicability in practice. In this work, we study robust continual graph learning, where models must simultaneously handle catastrophic forgetting and noisy supervision in evolving graph data. We show that label noise introduces a new failure mode catastrophic remembering, where models persistently reinforce corrupted knowledge across tasks. To address these challenges, we propose a Unified Flow-Oriented framework (UFO). First, UFO models conditional feature distributions via flow-based generative modeling and produces replay representations, mitigating forgetting without storing historical data. Second, UFO estimates instance-level reliability scores to distinguish clean from noisy nodes, reducing the impact of corrupted supervision and alleviating catastrophic remembering. Extensive experiments on four benchmark graph datasets under varying noise ratios demonstrate that UFO consistently outperforms existing methods in both accuracy and forgetting metrics. Code is available at: <https://anonymous.4open.science/r/UFO>.

1 Introduction

Graphs in real-world applications are inherently dynamic and evolve over time [1]. In social, citation, and co-authorship networks, new entities and connections emerge continuously [2]. To handle this data stream, models must acquire new knowledge while preserving previously learned information. This necessity has established Continual Graph Learning (CGL) as a critical research area [3], focusing on learning from sequential graph data.

Despite its potential, CGL faces two primary obstacles. First, storage limitations and privacy concerns often make historical data inaccessible, leading to catastrophic forgetting [4]. Second, while most CGL models assume clean training labels, label noise is inevitable in practice. Real-world datasets often contain significant noise ratios, sometimes exceeding 30% [5]. On graphs, this noise is particularly destructive as the message-passing mechanism propagates and amplifies errors across neighborhoods [6]. This forces the model to memorize incorrect information, causing catastrophic remembering [7], where noise from new tasks disrupts the knowledge learning.

Current techniques rarely address both challenges simultaneously. Standard CGL methods rely on regularization or replay buffers to prevent forgetting [8], yet they neglect the quality of labels and fail to handle noise. Conversely, robust learning methods use sample selection or robust loss functions to mitigate noise [9], but they typically focus on the current task and ignore historical knowledge. Therefore, their effectiveness is strongly tied to accessible data, leaving knowledge learned from inaccessible data vulnerable to forgetting [10]. While a few hybrid approaches [7, 11, 12] have been

proposed for image data, they cannot perform as well on graphs. This is because noise propagates through the message-passing mechanism. The complex topology of graphs further complicates the distinction between noise and legitimate structural shifts [13].

To bridge this gap, we propose a unified perspective in which catastrophic forgetting and noise robustness can be addressed simultaneously. Our key insight is that both challenges can be mitigated by learning and leveraging the underlying feature distributions of the data. By aligning new observations with these distributions, the model can suppress noisy supervision, while the distributions themselves enable knowledge retention without storing historical data.

Concretely, we replace explicit data storage with a generative distribution model. This model synthesizes representative features of past tasks for replay, preserving performance while avoiding the need to retain sensitive or large-scale historical data. At the same time, we estimate the reliability of incoming nodes based on their consistency with the learned distributions, allowing the model to down-weight noisy or corrupted samples during training.

Building on this idea, we propose **UFO**, a unified framework for robust continual graph learning without historical data storage. UFO models conditional feature distributions to generate replay representations, effectively mitigating catastrophic forgetting. To handle label noise, UFO incorporates an instance-level adaptation mechanism that assigns importance weights to nodes based on their alignment with the learned feature space, ensuring that reliable samples dominate model updates. In addition, a knowledge preservation strategy constrains representation drift across tasks, maintaining both structural and semantic consistency over time.

In summary, our main contributions are as follows:

- We introduce the problem of robust continual graph learning with label noise, and identify a new failure mode, catastrophic remembering, caused by the accumulation of corrupted supervision.
- We propose UFO, a unified framework that combines distribution-based feature replay and instance-level reliability estimation to address forgetting and noisy labels without storing historical data.
- We conduct extensive experiments on multiple benchmark datasets, demonstrating that UFO consistently improves both predictive performance and robustness under varying noise levels.

2 Related Work

2.1 Continual Graph Learning

Continual graph learning [14] is a paradigm that enables models to learn from evolving graphs while mitigating catastrophic forgetting. Existing approaches are divided into three families: (1) Regularization-based methods introduce a penalty term in the loss function to constrain the updates of crucial parameters. Early studies like LwF [15] learn the soft labels from the old model and TWP [16] preserves the topological aggregation of previous graphs. (2) Experience replay-based methods store or generate representative samples from previous tasks, e.g., DMSG [17] takes into account memory diversity through selection and generation. DSLR [18] introduces the coverage-based diversity and graph structure learning. (3) Parameter isolation-based methods use different parameters to different tasks, so that learning a new task has less effect on old tasks. HPNs [8] dynamically learns different levels of prototypes. However, all these methods are dependent on clean supervision, which limits their practicality in real-world scenarios [19]. In this work, we consider a more challenging problem in robust continual graph learning: how to learn from sequential tasks under corrupted supervision when historical data are inaccessible? This requires the model to preserve correct knowledge from seen tasks while avoiding the reinforcement of corrupted information.

2.2 Graph Learning with Label Noise

Learning with label noise [20] focuses on training models with corrupted data. There have been many efforts to enhance robustness, such as robust loss design [21], label correction [22], and sample selection [23]. For example, SCE [24] improves robustness by combining cross entropy with a reverse cross entropy. Bootstrap [25] replaces the target labels with a combination of their predicted labels. Recent works have extended these ideas to graph learning. CLNode [26] proposes a curricu-

lum learning framework for node classification with a multi-perspective difficulty measurer. TFR [27] leverages a backbone GNN and a decoder GNN to reconstruct topological features to maximize mutual information. TSS [28] utilizes graph topology to progressively select confident nodes and trains the model from easy to hard. However, existing methods focus on the current task and overlook real-world dynamic graph environments, where historical graph data may be unavailable due to privacy or storage constraints, making previously learned knowledge vulnerable to forgetting.

3 Problem Statement

3.1 Notations

Consider a sequence of n tasks $\{\mathcal{T}_1, \mathcal{T}_2, \dots, \mathcal{T}_t, \dots, \mathcal{T}_n\}$. Each task \mathcal{T}_t is defined on a graph $\mathcal{G}_t = \{\mathcal{V}_t, \mathcal{E}_t\}$, where \mathcal{V}_t is the node set and \mathcal{E}_t is the edge set. The graph structure is represented by the adjacency matrix $A_t \in \mathbb{R}^{N_t \times N_t}$, where $N_t = |\mathcal{V}_t|$. Each node $v_i \in \mathcal{V}_t$ has an input feature $h_i^{(0)}$ and an observed label y_i . During the training stage of task \mathcal{T}_t , the node set \mathcal{V}_t is divided into a training set \mathcal{V}_t^{tr} , a validation set \mathcal{V}_t^{val} , and a test set \mathcal{V}_t^{te} . The observed labels may be noisy in \mathcal{V}_t^{tr} and clean in \mathcal{V}_t^{val} and \mathcal{V}_t^{te} . Formally, our objective is to learn sequential tasks under corrupted supervision while preserving previously learned knowledge: $\min_{\Theta_t} \frac{1}{t} \sum_{j=1}^t \mathcal{L}_j(\Theta_t)$, where Θ_t refers to the model parameters for the t -th task.

3.2 Preliminary

Given an input $x \in \mathcal{X}$ and a latent variable $z \in \mathcal{Z}$, a normalizing flow [29, 30] defines an invertible mapping $f : \mathcal{X} \rightarrow \mathcal{Z}$ that transforms the original distribution into a base distribution, such as a standard Gaussian distribution. Here, $z = f(x)$ and $x = f^{-1}(z)$. By the change of variables formula, the likelihood of x can be written as:

$$p_X(x) = p_Z(z) \left| \det \frac{\partial f(x)}{\partial x} \right|, \quad (1)$$

where $\left| \det \frac{\partial f(x)}{\partial x} \right|$ is the absolute Jacobian determinant of the transformation f . In addition, let $y \in \mathcal{Y}$ be the class label, and the flow can be extended to the conditional setting [31]. The invertible mapping becomes $f : \mathcal{X} \times \mathcal{Y} \rightarrow \mathcal{Z}$, where $z = f(x, y)$ and $x = f^{-1}(z, y)$. We can express the conditional density of x by:

$$p_{X|Y}(x | y) = p_Z(z) \left| \det \frac{\partial f(x, y)}{\partial x} \right|. \quad (2)$$

In general, a single transformation is not flexible enough to model a complex distribution [32]. Therefore, f is defined as a composition of K simple invertible transformations: $f = f_K \circ \dots \circ f_1$. The \circ denotes function composition. Based on Eq. (2), the conditional log-likelihood of x under label y is:

$$\log p_{X|Y}(x | y) = \log p_Z(z) + \sum_{k=1}^K \log \left| \det \frac{\partial z_k}{\partial z_{k-1}} \right|, \quad (3)$$

where z_k is the intermediate variable after the k -th transformation.

4 Methodology

This section introduces UFO, as illustrated in Figure 1. The following sections describe three related modules that work together. First, Section 4.1 introduces the modeling of flow, which maps feature distributions into a shared standard Gaussian latent space and uses the learned distributions to generate replay representations for earlier tasks. Second, Section 4.2 presents the instance-level adaptation mechanism. At task \mathcal{T}_t , the current flow f_t assigns dynamic scores to instances according to their alignment with the task distribution, reducing the effect of noisy supervision in \mathcal{L}_{new} . The frozen flow f_{t-1} scores generated replay features in the historical feature space, down-weighting low-likelihood samples in \mathcal{L}_{old} . Finally, Section 4.3 introduces graph knowledge preservation, which constrains structural and semantic consistency across tasks.

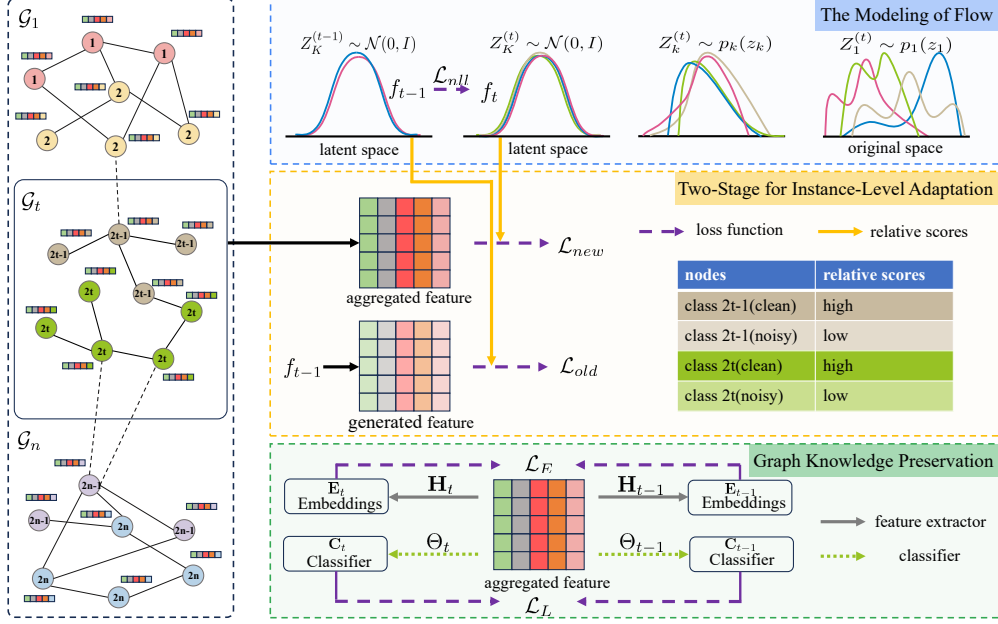


Figure 1: The framework of UFO: (1) The flow models feature distributions over sequential graphs and generates features for previous tasks. (2) Relative scores are computed using f_t and f_{t-1} , and are used to modulate \mathcal{L}_{new} and \mathcal{L}_{old} for instance-level adaptation. (3) Knowledge preservation constraints maintain structural and semantic consistency across tasks.

4.1 The Modeling of Flow

Flows are a type of powerful generative models. They learn an invertible mapping from a target data distribution to a simple latent distribution [30]. Based on this property, we can replay graph features instead of storing exemplars, mitigating catastrophic forgetting while preserving data privacy to some extent. Since graph features from different classes follow distinct distributions [33], we employ a conditional normalizing flow to model feature distributions for feature replay.

To learn informative graph representations, we employ the graph neural network proposed by [34] as the graph encoder. Given the neighborhood set $\mathcal{N}(v)$ of node v , the embedding $h_v^{(l)}$ at the l -th layer is calculated as follows:

$$h_{\mathcal{N}(v)}^{(l)} = \text{AGGREGATE}^{(l)}(\{h_u^{(l-1)}, \forall u \in \mathcal{N}(v)\}), \quad (4)$$

$$h_v^{(l)} = \sigma\left(W^{(l)} \cdot \text{CONCAT}(h_v^{(l-1)}, h_{\mathcal{N}(v)}^{(l)})\right), \quad (5)$$

where $W^{(l)}$ is the learnable parameter at the l -th layer. σ is a nonlinear activation function. Eq. (5) shows that the embedding of node v is updated by combining its own representation with the aggregated information from its neighbors. Following this message-passing mechanism, we construct the aggregated feature $x = \text{CONCAT}(h_v^{(l-1)}, h_{\mathcal{N}(v)}^{(l)})$.

When the observed labels are corrupted, the supervision signal becomes unreliable, as label noise weakens the true correlation between features and labels [35]. To capture the consistency, the flow models the conditional distribution $p_{X|Y}(x | y)$ for each class. The resulting likelihood is used to estimate the reliability of incoming nodes, while the learned distribution synthesizes replay features of past tasks without historical data storage.

For task \mathcal{T}_t , the flow adopts a shared standard Gaussian prior $\mathcal{N}(0, I)$ in the latent space and uses y as conditional information. It is trained on the current task \mathcal{T}_t by minimizing the negative log-likelihood:

$$\mathcal{L}_{nll} = - \sum_{v_i \in \mathcal{V}_t^{tr}} \log p_{X|Y}(x_i | y_i). \quad (6)$$

However, directly training the flow model on a single task leads to distributional bias. Inspired by [36], we incorporate a replay strategy to mitigate this issue. In particular, for each previous task \mathcal{T}_j with $1 \leq j < t$, latent variables \tilde{z}_i are sampled from the latent prior conditioned on labels \tilde{y}_i , resulting in the synthetic batch $\tilde{B}_j = \{(\tilde{z}_i, \tilde{y}_i)\}_{i=1}^b$, where b is the batch size. To avoid interference from the current task, we use the frozen previous flow to generate features $f_{t-1}^{-1}(\tilde{z}_i, \tilde{y}_i)$. Note that we use a tilde over the corresponding symbol to denote synthetic variables. The flow is then optimized using both aggregated and generated features:

$$\mathcal{L}_{nll} = - \sum_{v_i \in \mathcal{V}_t^{tr}} \log p_{X|Y}(x_i | y_i) - \sum_{(\tilde{z}_i, \tilde{y}_i) \in \tilde{B}_j} \log p_{X|Y}(f_{t-1}^{-1}(\tilde{z}_i, \tilde{y}_i) | \tilde{y}_i). \quad (7)$$

4.2 Two-Stage for Instance-Level Adaptation

In continual learning with label noise, corrupted labels can degrade the performance of graph neural networks and disrupt the model’s inherent stability, as noisy information may spread through graph structure [37, 38]. This effect can accumulate across tasks and cause catastrophic remembering, where the model retains incorrect knowledge from corrupted supervision. To this end, in the first stage, we calculate the conditional log-likelihood $r_i = \log p_{X|Y}(x_i | y_i)$ for instance-level adaptation. Since softmax is shift-invariant: $\text{softmax}(\mathbf{r}) = \text{softmax}(\mathbf{r} - m(\mathbf{r}))$, the relative scores \mathbf{s} are computed as:

$$m(\mathbf{r}) := \max_i r_i, \quad \mathbf{s} = b \cdot \text{softmax}(\mathbf{r} - m(\mathbf{r})), \quad (8)$$

where b is the batch size of the current task. Additionally, when learning a new task, the scores are smoothed to reduce outliers during early flow training and clipped to the interval $[\alpha, \beta]$: $s_i = \min(\beta, \max(\alpha, s_i))$.

In the next stage, we optimize two objectives. First, to fit the new task \mathcal{T}_t under noisy supervision, we reduce the negative impact of label noise using dynamic scores. The current flow f_t evaluates the conditional log-likelihood r_i to measure the alignment with the current task distribution, and r_i is further converted into the relative score s_i . The objective is formulated as follows:

$$\mathcal{L}_{ce}^{new} = \sum_{v_i \in \mathcal{V}_t^{tr}} s_i \ell_{ce}(C_t(H_t(v_i)), y_i), \quad (9)$$

where H_t is the feature extractor and C_t is the classifier. $\ell_{ce}(\cdot)$ denotes the cross-entropy loss. For previous task \mathcal{T}_j with $1 \leq j < t$, the second objective uses the synthetic batch \tilde{B}_j introduced above. The score \tilde{s}_i , computed by the frozen flow f_{t-1} , reflects the alignment of a generated feature with the learned historical feature space, reducing the influence of low-likelihood or out-of-distribution replay features caused by imperfect flow generation. The generative replay loss is defined as:

$$\mathcal{L}_{ce}^{old} = \sum_{(\tilde{z}_i, \tilde{y}_i) \in \tilde{B}_j} \tilde{s}_i \ell_{ce}(C_t(f_{t-1}^{-1}(\tilde{z}_i, \tilde{y}_i)), \tilde{y}_i). \quad (10)$$

4.3 Graph Knowledge Preservation

As a sequence of graphs arrives, the original feature space gradually shifts, which alters the representations learned from previous tasks and weakens the stability of the latent space [15]. Since the flow relies on a stable feature space to model distributions, we preserve graph knowledge to control the shifts and maintain the learned structural and semantic information [39]. The embeddings are used to anchor the representation of the same node v_i :

$$\mathcal{L}_E = \sum_{v_i \in \mathcal{V}_t^{tr}} \|H_t(v_i) - H_{t-1}(v_i)\|_2^2, \quad (11)$$

where H_{t-1} is the feature extractor from task $t - 1$. Class semantic knowledge is encoded in the output distribution of the classifier, which reflects the relations among classes. Directly optimizing the current classifier may disrupt this previously learned knowledge. We therefore use the soft predictions from the frozen classifier C_{t-1} to guide the current classifier C_t . The two classifiers are evaluated with the same task head, and the Kullback–Leibler (KL) divergence is used for distillation:

$$\mathcal{L}_L = \sum_{v_i \in \mathcal{V}_t^{tr}} \tau^2 \text{KL}(\text{softmax}(C_{t-1}(H_{t-1}(v_i))/\tau) \parallel \text{softmax}(C_t(H_t(v_i))/\tau)), \quad (12)$$

Algorithm 1: Framework of UFO

Input: A sequence of n graphs $\{\mathcal{G}_1, \mathcal{G}_2, \dots, \mathcal{G}_n\}$, flow f , feature extractor H , classifier C

Output: Updated H_n and C_n

```
for  $t \leftarrow 1$  to  $n$  do
  if  $t = 1$  then
    Aggregate features  $\mathbf{x}_1$  from  $\mathcal{G}_1$ ;
    Train  $f_1$  on  $\mathbf{x}_1$  in Eq. (6);
    Train  $H_1$  and  $C_1$  on  $\mathcal{G}_1$  in Eq. (9);
  else
    Aggregate features  $\mathbf{x}_t$  from  $\mathcal{G}_t$ ;
    Generate features  $\tilde{\mathbf{x}}_{t-1}$  from  $f_{t-1}$ ;
    Train  $f_t$  on  $\mathbf{x}_t$  and  $\tilde{\mathbf{x}}_{t-1}$  in Eq. (7);
    Compute the relative scores from  $f_t$  and  $f_{t-1}$  in Eq. (8);
    Train  $H_t$  and  $C_t$  on  $\mathcal{G}_t$  and  $\tilde{\mathbf{x}}_{t-1}$  in Eqs. (9), (10), (13);
  end
end
```

where τ is a temperature parameter, and τ^2 is used to compensate for the $1/\tau^2$ scaling of the gradients. For the current task, the final objective for graph knowledge preservation is:

$$\mathcal{L}_{KP} = \alpha_E \mathcal{L}_E + \alpha_L \mathcal{L}_L, \quad (13)$$

where α_E and α_L are loss weights. The whole training process is summarized in Algorithm 1.

5 Experiments

5.1 Experimental Setup

Datasets and Implementation Details. We evaluate our method on four real-world datasets: Cora-Full [2], CS [40], WikiCS [41], and Photo [40]. More detailed statistics are provided in Appendix A.1. Following [42], we divide the classes into a sequence of tasks for each dataset, and split the nodes in each task into 60%, 20%, and 20% for training, validation, and testing, respectively. We add symmetric noise to a fraction of labels in the training set while keeping the validation and test sets clean. For each selected node, its label is replaced by a label uniformly sampled from the other classes within the same task. We also report the results under pair flipping label noise in Appendix B.1, where each selected label is flipped to a predefined paired class within the same task. The implementation and detailed settings are provided in Appendix A.4.

Baselines. Since there is no existing method specifically designed for our problem, we summarize eight baselines into two categories. The first category includes well-known continual learning methods, such as LwF [15], ERGNN [43], DSLR [18], and DMSG [17]. To adapt these methods to noisy labels, we introduce the SCE [24] loss during training. The second category consists of methods designed for noisy label learning, including SCE, CLNode [26], TSS [28], and TFR [27]. Since these methods are not originally designed for continual learning, we adopt the CM strategy from ERGNN to construct a memory buffer to prevent catastrophic forgetting. For consistency, we store 10 samples per class and use a two-layer GCN as the backbone. Moreover, two standard reference settings are included. Joint is an offline upper-bound reference with access to data from all tasks, while bare model is the backbone GCN without additional strategies, serving as a lower-bound reference. A full description of the baseline implementations is included in Appendix A.2.

Evaluation Metrics. To evaluate performance under varying noise levels in continual learning, following previous works [42, 44, 45], we use average accuracy and average forgetting as the primary metrics. Accuracy measures the average accuracy over tasks after learning the final task, and Forgetting measures the final retention of previous tasks. A higher accuracy or a higher forgetting suggests that the model has a better performance. The formal definitions of metrics are given in Appendix A.3.

Table 1: Average performance comparison on each dataset under noise ratios of $\{0\%, 15\%, 30\%\}$. The best performance is in **red**, and the second best is in **blue**.

Models	Accuracy \uparrow			Forgetting \uparrow		
	0%	15%	30%	0%	15%	30%
CoraFull						
Joint	90.40 \pm 0.10	75.82 \pm 0.12	62.45 \pm 0.27	-	-	-
Bare model	34.21 \pm 1.69	31.32 \pm 6.43	30.60 \pm 1.13	-61.91 \pm 3.50	-49.15 \pm 9.88	-36.00 \pm 1.09
LwF	60.32 \pm 0.77	55.25 \pm 2.14	50.87 \pm 1.54	-33.41 \pm 0.95	-24.84 \pm 2.82	-15.57 \pm 1.43
ERGNN	77.74 \pm 0.15	40.91 \pm 0.34	33.94 \pm 0.58	-4.62\pm0.37	-33.06 \pm 0.40	-32.94 \pm 0.37
DSLRL	74.23 \pm 0.90	62.09 \pm 1.62	51.06 \pm 0.99	-14.47 \pm 0.84	-11.75 \pm 1.46	-8.98 \pm 0.75
DMSG	<u>78.04\pm0.56</u>	<u>67.20\pm0.82</u>	<u>59.71\pm1.30</u>	-13.20 \pm 0.66	<u>-10.65\pm0.81</u>	<u>-7.68\pm0.85</u>
SCE	39.30 \pm 0.15	41.27 \pm 1.21	34.41 \pm 1.77	-56.65 \pm 0.28	-42.06 \pm 1.45	-35.08 \pm 2.14
CLNode	78.01 \pm 0.18	30.12 \pm 0.81	27.13 \pm 0.22	<u>-5.06\pm0.31</u>	-53.95 \pm 0.37	-55.91 \pm 0.52
TSS	75.02 \pm 0.57	27.61 \pm 1.89	25.27 \pm 1.69	-9.20 \pm 1.30	-52.97 \pm 1.22	-47.19 \pm 1.38
TFR	49.08 \pm 0.61	36.08 \pm 1.35	26.89 \pm 1.36	-45.95 \pm 0.72	-45.92 \pm 0.61	-42.35 \pm 1.09
UFO	81.78\pm0.85	80.71\pm0.08	77.77\pm1.04	-6.35 \pm 1.10	-6.33\pm2.25	-7.10\pm1.27
CS						
Joint	97.00 \pm 0.10	67.43 \pm 4.15	51.06 \pm 1.83	-	-	-
Bare model	61.22 \pm 0.10	62.83 \pm 0.07	53.04 \pm 0.03	-45.55 \pm 0.02	-28.98 \pm 0.01	-25.10 \pm 0.21
LwF	92.51 \pm 4.10	53.39 \pm 6.40	45.19 \pm 15.55	-5.49 \pm 4.78	-40.94 \pm 8.02	-32.99 \pm 13.22
ERGNN	94.40 \pm 0.14	57.82 \pm 2.86	47.73 \pm 3.43	-3.26 \pm 0.29	-20.09 \pm 6.03	-11.67 \pm 0.85
DSLRL	<u>96.47\pm0.80</u>	<u>77.67\pm0.45</u>	<u>68.10\pm1.80</u>	<u>-2.01\pm0.88</u>	-12.98 \pm 1.59	-2.29 \pm 2.39
DMSG	<u>93.87\pm1.14</u>	70.46 \pm 3.67	57.55 \pm 8.96	-4.24 \pm 1.43	<u>-6.34\pm4.45</u>	7.13\pm9.74
SCE	78.90 \pm 7.20	58.42 \pm 8.09	46.00 \pm 6.30	-22.48 \pm 8.69	-33.80 \pm 11.78	-29.68 \pm 5.30
CLNode	93.84 \pm 0.32	51.80 \pm 1.52	57.89 \pm 1.22	-3.84 \pm 0.47	-55.76 \pm 1.90	-47.60 \pm 1.36
TSS	79.62 \pm 5.16	55.28 \pm 9.70	48.12 \pm 6.16	-14.29 \pm 8.06	-41.88 \pm 12.52	-36.27 \pm 8.29
TFR	94.11 \pm 1.98	28.33 \pm 9.63	28.81 \pm 8.76	-3.43 \pm 2.58	-48.21 \pm 15.95	-11.52 \pm 6.81
UFO	97.29\pm0.29	92.21\pm0.43	81.46\pm0.43	-1.30\pm0.27	0.06\pm1.34	<u>3.14\pm0.20</u>
WikiCS						
Joint	92.70 \pm 0.40	90.88 \pm 0.40	86.41 \pm 3.01	-	-	-
Bare model	77.72 \pm 4.51	68.95 \pm 6.56	65.24 \pm 7.98	-17.67 \pm 5.91	-21.10 \pm 3.59	-15.06 \pm 11.64
LwF	<u>88.75\pm1.54</u>	74.06 \pm 4.37	62.76 \pm 4.96	<u>-4.72\pm2.09</u>	-20.50 \pm 6.35	-20.08 \pm 6.83
ERGNN	86.58 \pm 0.36	52.77 \pm 3.69	48.62 \pm 6.77	-6.54 \pm 0.37	-44.23 \pm 10.28	-39.28 \pm 2.36
DSLRL	82.71 \pm 0.71	70.35 \pm 2.87	61.74 \pm 1.39	-8.65 \pm 0.44	-12.93 \pm 2.34	<u>-8.49\pm2.93</u>
DMSG	83.69 \pm 1.55	<u>82.18\pm2.34</u>	<u>66.11\pm5.12</u>	-10.84 \pm 1.48	<u>-9.69\pm2.01</u>	-18.36 \pm 10.72
SCE	76.26 \pm 0.40	65.59 \pm 2.69	52.77 \pm 3.74	-21.16 \pm 0.81	-29.05 \pm 4.66	-24.16 \pm 4.64
CLNode	80.25 \pm 2.05	52.31 \pm 1.36	55.63 \pm 2.62	-14.70 \pm 2.43	-49.74 \pm 1.13	-45.26 \pm 2.78
TSS	73.99 \pm 0.55	52.14 \pm 6.47	49.80 \pm 6.78	-13.69 \pm 1.05	-42.47 \pm 7.24	-40.11 \pm 10.63
TFR	83.37 \pm 0.82	60.88 \pm 7.36	42.42 \pm 2.64	-8.04 \pm 3.94	-14.95 \pm 10.51	-35.46 \pm 1.84
UFO	93.36\pm0.01	93.29\pm0.08	83.10\pm0.89	-0.69\pm0.07	-0.66\pm0.10	-8.27\pm1.16
Photo						
Joint	96.90 \pm 0.80	93.24 \pm 0.72	85.87 \pm 2.34	-	-	-
Bare model	65.75 \pm 0.01	49.64 \pm 0.02	49.63 \pm 0.05	-38.78 \pm 0.07	-30.02 \pm 0.04	-22.34 \pm 0.06
LwF	80.03 \pm 19.44	79.21 \pm 9.37	63.36 \pm 1.30	-18.51 \pm 18.04	-12.05 \pm 19.43	-17.23 \pm 16.98
ERGNN	95.49 \pm 0.14	42.62 \pm 11.31	53.00 \pm 17.22	-5.37 \pm 7.26	<u>-0.48\pm1.65</u>	-30.88 \pm 11.94
DSLRL	<u>97.36\pm0.14</u>	<u>87.70\pm1.60</u>	<u>69.62\pm3.95</u>	-1.28 \pm 0.36	-11.90 \pm 2.64	-18.56 \pm 8.21
DMSG	49.58 \pm 0.02	57.11 \pm 7.66	50.27 \pm 0.89	<u>-0.31\pm0.15</u>	-23.91 \pm 12.93	<u>0.77\pm1.24</u>
SCE	63.85 \pm 5.86	47.63 \pm 5.82	57.59 \pm 11.41	-42.02 \pm 7.47	-37.85 \pm 20.60	-10.61 \pm 15.30
CLNode	89.31 \pm 9.31	57.28 \pm 11.90	59.86 \pm 4.83	-8.53 \pm 11.61	-50.99 \pm 14.67	-46.61 \pm 6.51
TSS	61.44 \pm 11.38	62.42 \pm 8.31	55.51 \pm 10.22	-34.36 \pm 19.57	-27.04 \pm 20.64	-35.44 \pm 4.19
TFR	73.87 \pm 4.70	51.82 \pm 4.04	46.42 \pm 1.78	-28.18 \pm 6.61	-28.01 \pm 12.53	-32.90 \pm 1.15
UFO	98.07\pm0.04	96.04\pm0.25	93.40\pm0.86	-0.22\pm0.06	-0.17\pm0.49	1.61\pm0.99

5.2 Comparison Study

Table 1 shows that UFO performs better on four datasets under varying noise ratios. As the noise ratio increases, all models show lower average accuracy, while forgetting first decreases and then increases. This is because noise may already hurt the model at an early stage, preventing it from learning true knowledge well, so the later performance change becomes less obvious. Existing CGL methods mainly focus on mitigating catastrophic forgetting, so their average forgetting remains relatively stable. On CoraFull, when the noise ratio increases from 0% to 30%, the accuracy of DSLR decreases by 23.17%, while its forgetting increases by 5.49%. However, among graph learning with

label noise methods, the forgetting of CLNode and TSS decreases by 50.85% and 37.99%. This may be related to its higher early accuracy, and continuously arriving noisy labels further affect the stability of the model. In contrast, UFO shows smaller changes in both accuracy and forgetting on all four datasets, demonstrating stronger robustness under noisy conditions.

To further analyze the overall behavior of different models, we visualize the performance matrices on CoraFull under the 30% noise setting. As shown in Figure 2, darker colors indicate higher accuracy. For LwF and ERGNN, the dark regions are concentrated along the diagonal and the colors become lighter for earlier tasks. Under noisy labels, DSLR and DMSG show relatively uniform but lighter color distributions. In contrast, UFO shows a more stable and darker matrix, demonstrating that it not only preserves knowledge but also reduces the accumulation of corrupted supervision, which achieves a better balance between catastrophic forgetting and catastrophic remembering. Due to space limitations, more comparisons are provided in Appendix B.2.

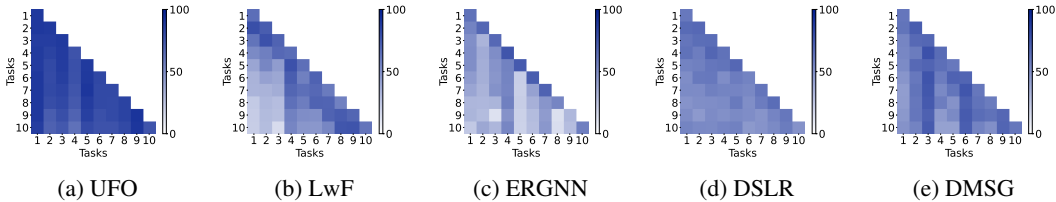


Figure 2: Performance matrices on CoraFull with 30% noise.

5.3 Ablation Study

To further analyze the effectiveness of each component, we conduct an ablation study on CoraFull and CS with different noise ratios. We consider the bare model (BM), knowledge preservation (KP), relative scores for the new task (NS) and old task (OS), and the replay mechanism (R). The results in Table 2 show that: (1) KP enables the BM to achieve better performance by preserving previous knowledge and reducing feature drift. (2) When NS is further introduced, the model achieves higher accuracy in several noise ratios, especially under 15% noise. (3) R brings clear gains, e.g., improving the forgetting value on CoraFull with 30% noise from -53.92% to -7.93% . (4) After adding OS, UFO achieves the best overall performance across varying noise levels. This suggests that OS helps filter low-quality features generated by the flow model.

Table 2: Ablation study of our UFO. The best performance is highlighted in **red**.

Metric	Noise	BM	BM+KP	BM+KP+NS	BM+KP+NS+R	UFO
CoraFull						
Accuracy↑	0%	33.71±4.74	47.14±0.40	47.07±0.60	53.16±2.48	81.78±0.85
	15%	34.02±0.58	39.19±0.47	40.78±0.49	51.21±0.12	80.71±0.08
	30%	29.02±2.34	33.22±1.00	33.27±0.46	46.65±1.01	77.77±1.04
Forgetting↑	0%	-62.09±5.34	-47.37±0.46	-47.39±0.71	-6.39±2.32	-6.35±1.10
	15%	-47.04±0.37	-53.46±0.62	-51.78±0.61	-6.57±0.79	-6.33±2.25
	30%	-38.10±2.53	-53.98±1.17	-53.92±0.55	-7.93±1.08	-7.10±1.27
CS						
Accuracy↑	0%	61.22±0.10	93.53±0.54	92.31±0.48	96.16±0.51	97.29±0.29
	15%	62.83±0.07	87.15±1.10	89.18±0.36	90.32±1.12	92.21±0.43
	30%	53.04±0.03	69.91±3.80	67.11±3.60	78.65±3.44	81.46±0.43
Forgetting↑	0%	-45.55±0.02	-5.59±0.62	-7.09±0.59	-2.36±0.60	-1.30±0.27
	15%	-28.98±0.01	-1.99±1.25	0.29±0.58	-0.22±1.22	0.06±1.34
	30%	-25.10±0.21	-8.14±4.58	-12.28±4.20	-0.32±4.19	3.14±0.20

5.4 Hyperparameter

We evaluate the sensitivity to the number of flows in Figure 3. As observed, the performance remains stable with 0% noise, indicating a shallow or moderate flow is sufficient for clean distributions. When the noise ratio increases to 30%, accuracy and forgetting reach their best levels around 9–12

flows. With the number of flows further increasing to 13, the results drop clearly. This suggests that a moderate flow depth provides a better balance for robust continual learning, while an overly deep flow increases optimization difficulty.

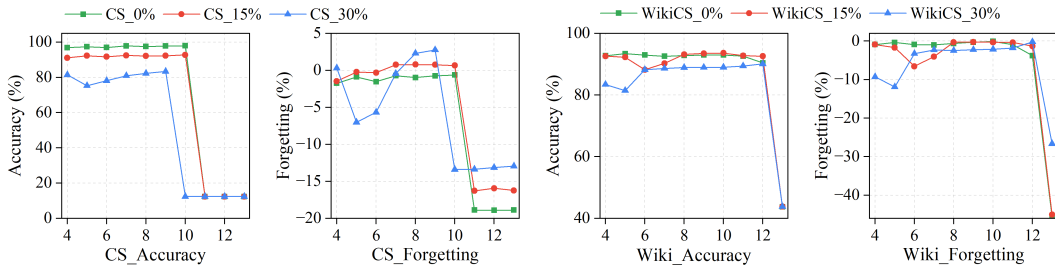


Figure 3: Sensitivity analysis for the number of flows with 0%, 15%, and 30% noise.

5.5 Visualization

To analyze the evolution of clean and noisy nodes, we visualize the embeddings of the classes from the first task (classes 0, 1, and 2) on CS in Figure 4. The three subfigures show the embeddings learned by UFO on sequential CS with 0%, 15%, and 30% noise. The 0% noise setting provides a clean reference, where the embeddings form distinct clusters with minimal overlap. As the noise ratio increases to 15%, 30%, we can observe that noisy nodes in UFO are mainly located near the boundary or the outer region of each cluster. Comparing Task 1 and Task 5, the embeddings of old classes show less drift and preserve relatively stable structures. This suggests that UFO can preserve knowledge and maintain robust representations under noisy supervision. The complete visualization results for UFO and Joint are provided in Appendix B.3.

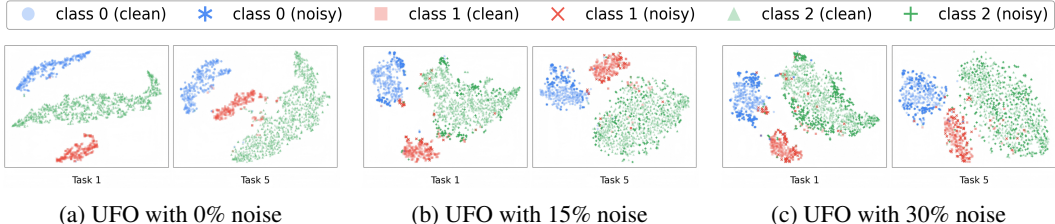


Figure 4: t-SNE visualization of the evolution of embeddings for classes 0, 1, and 2 on sequential CS.

6 Limitations

This work has two limitations. First, UFO performs replay in the feature space and does not explicitly reconstruct the original graph topology, such as historical edges and neighborhoods. This may limit the ability of feature replay to fully recover structural knowledge from previous tasks. Second, UFO relies on the configuration of the flow model. An overly deep flow can increase optimization difficulty and computational cost. Thus, the number of flow layers and related hyperparameters need to be selected carefully in practice.

7 Conclusion

In this paper, we study a more realistic robust continual graph learning scenario and identify a new failure mode caused by the accumulation of noisy supervision. To jointly address these challenges, we propose UFO, a unified flow-oriented framework. UFO uses normalizing flows to conditionally model feature distributions for replay and estimate instance-level reliability under corrupted supervision. Furthermore, we introduce graph knowledge preservation to constrain structural and semantic

consistency. Experimental results demonstrate the superiority of UFO in improving performance and robustness under varying noise levels.

References

- [1] Feng Xia, Ciyuan Peng, Jing Ren, et al. Graph learning. *Foundations and Trends® in Signal Processing*, pages 362–519, 2026.
- [2] Aleksandar Bojchevski and Stephan Günnemann. Deep gaussian embedding of graphs: Unsupervised inductive learning via ranking. In *International Conference on Learning Representations*, 2018.
- [3] James Kirkpatrick, Razvan Pascanu, Neil C. Rabinowitz, et al. Overcoming catastrophic forgetting in neural networks. *Proceedings of the National Academy of Sciences*, pages 3521–3526, 2017.
- [4] Jialu Li, Yu Wang, Pengfei Zhu, et al. What matters in graph class incremental learning? An information preservation perspective. In *Proceedings of the 38th International Conference on Neural Information Processing Systems*, pages 26195–26223, 2024.
- [5] Hwanjun Song, Minseok Kim, and Jae-Gil Lee. SELFIE: Refurbishing unclean samples for robust deep learning. In *Proceedings of the 36th International Conference on Machine Learning*, pages 5907–5915, 2019.
- [6] Zhonghao Wang, Danyu Sun, Sheng Zhou, et al. NoisyGL: A comprehensive benchmark for graph neural networks under label noise. In *Proceedings of the 38th International Conference on Neural Information Processing Systems*, pages 38142–38170, 2024.
- [7] Kunlun Xu, Haozhuo Zhang, Yu Li, et al. Mitigate catastrophic remembering via continual knowledge purification for noisy lifelong person re-identification. In *Proceedings of the 32nd ACM International Conference on Multimedia*, pages 5790–5799, 2024.
- [8] Xikun Zhang, Dongjin Song, and Dacheng Tao. Hierarchical prototype networks for continual graph representation learning. *IEEE Transactions on Pattern Analysis and Machine Intelligence*, pages 4622–4636, 2023.
- [9] Bo Han, Quanming Yao, Xingrui Yu, et al. Co-teaching: robust training of deep neural networks with extremely noisy labels. In *Proceedings of the 32nd International Conference on Neural Information Processing Systems*, pages 8536–8546, 2018.
- [10] Daiqing Qi, Handong Zhao, Xiaowei Jia, and Sheng Li. Revealing an overlooked challenge in class-incremental graph learning. *Transactions on Machine Learning Research*, 2024.
- [11] Xuemei Cao, Hanlin Gu, Xin Yang, et al. ErrorEraser: Unlearning data bias for improved continual learning. In *Proceedings of the 31st ACM SIGKDD Conference on Knowledge Discovery and Data Mining V.2*, pages 119–130, 2025.
- [12] Chris Dongjoo Kim, Jinseo Jeong, Sangwoo Moon, et al. Continual learning on noisy data streams via self-purified replay. In *Proceedings of the IEEE/CVF International Conference on Computer Vision*, pages 537–547, 2021.
- [13] Kailai Li, Jiawei Sun, Jiong Lou, Zhanbo Feng, Hefeng Zhou, Chentao Wu, Guangtao Xue, Wei Zhao, and Jie Li. Leveraging peer-informed label consistency for robust graph neural networks with noisy labels. In James Kwok, editor, *Proceedings of the Thirty-Fourth International Joint Conference on Artificial Intelligence, IJCAI-25*, pages 5598–5606. International Joint Conferences on Artificial Intelligence Organization, 8 2025. Main Track.
- [14] Xikun Zhang, Dongjin Song, and Dacheng Tao. Continual learning on graphs: Challenges, solutions, and opportunities. *arXiv preprint arXiv:2402.11565*, 2024.
- [15] Zhizhong Li and Derek Hoiem. Learning without forgetting. *IEEE Transactions on Pattern Analysis and Machine Intelligence*, 40(12):2935–2947, 2017.

- [16] Huihui Liu, Yiding Yang, and Xinchao Wang. Overcoming catastrophic forgetting in graph neural networks. *Proceedings of the AAAI Conference on Artificial Intelligence*, pages 8653–8661, 2021.
- [17] Ziyue Qiao, Junren Xiao, Qingqiang Sun, et al. Towards continuous reuse of graph models via holistic memory diversification. In *International Conference on Learning Representations*, 2025.
- [18] Seungyoon Choi, Wonjoong Kim, Sungwon Kim, et al. DSLR: Diversity enhancement and structure learning for rehearsal-based graph continual learning. In *Proceedings of the ACM Web Conference 2024*, pages 733–744, 2024.
- [19] Mengmeng Sheng, Zeren Sun, Tianfei Zhou, et al. CA2C: A prior-knowledge-free approach for robust label noise learning via asymmetric co-learning and co-training. In *Proceedings of the IEEE/CVF International Conference on Computer Vision*, pages 901–911, 2025.
- [20] Hwanjun Song, Minseok Kim, Dongmin Park, et al. Learning from noisy labels with deep neural networks: A survey. *IEEE Transactions on Neural Networks and Learning Systems*, pages 8135–8153, 2023.
- [21] Zhilu Zhang and Mert R Sabuncu. Generalized cross entropy loss for training deep neural networks with noisy labels. In *Proceedings of the 32nd International Conference on Neural Information Processing Systems*, pages 8792–8802, 2018.
- [22] Kun Yi and Jianxin Wu. Probabilistic end-to-end noise correction for learning with noisy labels. In *Proceedings of the IEEE/CVF conference on computer vision and pattern recognition*, pages 7017–7025, 2019.
- [23] Xingrui Yu, Bo Han, Jiangchao Yao, et al. How does disagreement help generalization against label corruption? In *International Conference on Machine Learning*, pages 7164–7173, 2019.
- [24] Yisen Wang, Xingjun Ma, Zaiyi Chen, et al. Symmetric cross entropy for robust learning with noisy labels. In *Proceedings of the IEEE/CVF international conference on computer vision*, pages 322–330, 2019.
- [25] Scott Reed, Honglak Lee, Dragomir Anguelov, et al. Training deep neural networks on noisy labels with bootstrapping. *arXiv preprint arXiv:1412.6596*, 2014.
- [26] Xiaowen Wei, Xiuwen Gong, Yibing Zhan, et al. CLNode: Curriculum learning for node classification. In *Proceedings of the 16th ACM International Conference on Web Search and Data Mining*, pages 670–678, 2023.
- [27] Zhonghao Wang, Yuanchen Bei, Sheng Zhou, et al. Learning from graph: Mitigating label noise on graph through topological feature reconstruction. In *Proceedings of the 34th ACM International Conference on Information and Knowledge Management*, pages 3261–3270, 2025.
- [28] Yuhao Wu, Jiangchao Yao, Xiaobo Xia, et al. Mitigating label noise on graphs via topological sample selection. In *Proceedings of the 41st International Conference on Machine Learning*, pages 53944–53972, 2024.
- [29] Danilo Rezende and Shakir Mohamed. Variational inference with normalizing flows. In *Proceedings of the 32nd International Conference on Machine Learning*, pages 1530–1538, 2015.
- [30] Laurent Dinh, Jascha Sohl-Dickstein, and Samy Bengio. Density estimation using real NVP. In *International Conference on Learning Representations*, 2017.
- [31] Pavel Izmailov, Polina Kirichenko, Marc Finzi, and Andrew Gordon Wilson. Semi-supervised learning with normalizing flows. In Hal Daumé III and Aarti Singh, editors, *Proceedings of the 37th International Conference on Machine Learning*, volume 119 of *Proceedings of Machine Learning Research*, pages 4615–4630, 13–18 Jul 2020.
- [32] George Papamakarios, Eric Nalisnick, Danilo Jimenez Rezende, et al. Normalizing flows for probabilistic modeling and inference. *Journal of Machine Learning Research*, (57):1–64, 2021.

- [33] Jiawei Gu, Ziyue Qiao, and Xiao Luo. Neubm: Mitigating model bias in graph neural networks through neutral input calibration. In *Proceedings of the 34th International Joint Conference on Artificial Intelligence*, pages 2829–2837, 2025.
- [34] William L Hamilton, Rex Ying, and Jure Leskovec. Inductive representation learning on large graphs. In *Proceedings of the 31st International Conference on Neural Information Processing Systems*, pages 1025–1035, 2017.
- [35] Hao Cheng, Zhaowei Zhu, Xingyu Li, et al. Learning with instance-dependent label noise: A sample sieve approach. In *International Conference on Learning Representations*, 2021.
- [36] Abudukelimu Wuerkaixi, Sen Cui, Jingfeng Zhang, et al. Accurate forgetting for heterogeneous federated continual learning. In *The 12th International Conference on Learning Representations*, 2024.
- [37] Enyan Dai, Charu Aggarwal, and Suhang Wang. NRGNN: Learning a label noise resistant graph neural network on sparsely and noisily labeled graphs. In *Proceedings of the 27th ACM SIGKDD Conference on Knowledge Discovery & Data Mining*, pages 227–236, 2021.
- [38] Kuan Zhang, Chengliang Chai, Jingzhe Xu, et al. Handling label noise via instance-level difficulty modeling and dynamic optimization. In *Proceedings of the 39th International Conference on Neural Information Processing Systems*, pages 46667–46696, 2025.
- [39] Yiding Yang, Jiayan Qiu, Mingli Song, et al. Distilling knowledge from graph convolutional networks. In *Proceedings of the IEEE/CVF Conference on Computer Vision and Pattern Recognition*, pages 7074–7083, 2020.
- [40] Oleksandr Shchur, Maximilian Mumme, Aleksandar Bojchevski, and Stephan Günnemann. Pitfalls of graph neural network evaluation. *arXiv preprint arXiv:1811.05868*, 2018.
- [41] Péter Mernyei and Cătălina Cangea. Wiki-CS: A wikipedia-based benchmark for graph neural networks. *arXiv preprint arXiv:2007.02901*, 2020.
- [42] Xikun Zhang, Dongjin Song, and Dacheng Tao. CGLB: benchmark tasks for continual graph learning. In *Proceedings of the 36th International Conference on Neural Information Processing Systems*, pages 13006–13021, 2022.
- [43] Fan Zhou and Chengtai Cao. Overcoming catastrophic forgetting in graph neural networks with experience replay. *Proceedings of the AAAI Conference on Artificial Intelligence*, pages 4714–4722, 2021.
- [44] Ting Wu, Jingyi Liu, Rui Zheng, et al. Enhancing contrastive learning with noise-guided attack: Towards continual relation extraction in the wild. In *Proceedings of the 62nd Annual Meeting of the Association for Computational Linguistics (Volume 1: Long Papers)*, pages 2227–2239, 2024.
- [45] Yinlin Zhu, Miao Hu, and Di Wu. Federated continual graph learning. In *Proceedings of the 31st ACM SIGKDD Conference on Knowledge Discovery and Data Mining V.2*, pages 4203–4213, 2025.

A Implementation Details

A.1 Datasets

In our experiments, we evaluate our method on four widely used graph datasets.

- **CoraFull** [2] is an academic citation network with 70 classes, where nodes denote academic papers and edges denote citation links between papers.
- **CS** [40] is an author collaboration network extracted from the Microsoft Academic Graph. In this dataset, each node represents an author, and an edge connects two authors who have co-authored a paper.
- **WikiCS** [41] is built from Wikipedia on computer science topics. It treats articles as nodes and hyperlinks as edges, and provides multiple predefined splits for reliable evaluation.
- **Photo** [40] is an Amazon co-purchase network from the photography category. Nodes represent products, and an edge is created when two items are frequently purchased together, reflecting implicit product relationships.

The statistics of these datasets are summarized in Table 3.

Table 3: Statistics of the Datasets.

Dataset	#Nodes	#Edges	#Features	#Classes	#Tasks
CoraFull	19,793	126,842	8,710	70	10
CS	18,333	163,788	6,805	15	5
WikiCS	11,701	431,726	300	10	5
Photo	7,650	238,162	745	8	4

A.2 Baselines

We compare our method with several state-of-the-art approaches from both continual graph learning and graph learning with label noise. The comparison methods are briefly introduced as follows.

- **Joint** trains the backbone GCN on all tasks simultaneously. Since it has access to the full task sequence, it is reported only as an upper-bound reference. This setting removes the influence of catastrophic forgetting and highlights the negative effect of noisy supervision.
- **Bare model** is the backbone GCN without any continual learning or robust strategy. It serves as a lower-bound reference, where the model is directly affected by catastrophic forgetting and catastrophic remembering.

Continual graph learning (adding an SCE loss term weighted by 0.5):

- **LwF** [15] is a regularization-based method that preserves knowledge from previous tasks by distilling soft targets from a historical model.
- **ERGNN** [43] selects representative nodes from previous tasks and replays them to reduce catastrophic forgetting in graph neural networks.
- **DSLRL** [18] improves experience replay by considering coverage-based diversity and graph structure learning, which helps preserve both feature and structural information.
- **DMSG** [17] improves memory replay by combining sample selection with generation, with explicit consideration of memory diversity in continual graph learning.

Graph learning with label noise (replaying 10 nodes per class):

- **SCE** [24] is a robust loss function that combines cross-entropy with reverse cross-entropy, making the model less sensitive to noisy labels.
- **CLNode** [26] uses curriculum learning for graph data, where node difficulty is estimated from multiple perspectives and the model is trained from easier to harder samples.

- **TSS** [28] leverages graph topology to iteratively select high-confidence nodes, allowing the model to learn from more reliable samples under label noise.
- **TFR** [27] introduces a dual-network framework with a backbone GNN and a decoder GNN, reconstructing topological features to enhance robustness via mutual information maximization.

A.3 Evaluation Metrics

We adopt two commonly used metrics in continual learning, namely accuracy and forgetting [42], to evaluate both the overall performance and robustness of the model across tasks. Formally, they are defined as:

$$\text{Accuracy} = \frac{1}{n} \sum_{i=1}^n A_{n,i}, \quad \text{Forgetting} = \frac{1}{n-1} \sum_{i=1}^{n-1} (A_{n,i} - A_{i,i}), \quad (14)$$

where n denotes the total number of tasks, and $A_{i,j}$ represents the test accuracy on task j after training up to task i . In particular, $A_{i,i}$ is the accuracy immediately after learning task i , while $A_{n,i}$ denotes its final accuracy after all tasks are learned.

A.4 Details Settings

We adopt the GCN as the backbone, with a hidden dimension of 256. Following [11, 42], the model is trained using the Adam optimizer with a learning rate of 0.005 for 200 epochs on each task. The flow model consists of 4 affine coupling layers and 4 permutation layers. The temperature parameter is set to $\tau = 2.71$, with $\alpha_E = 0.09$ and $\alpha_L = 0.06$. All results are reported as the mean and standard deviation over three independent runs, with implementation based on PyTorch 2.3.0 and CUDA 12.1 on a 48GB vGPU.

Table 4: Average performance comparison on CS under pair flipping noise. The best performance is in **red**, and the second best is in **blue**.

Models	Accuracy \uparrow			Forgetting \uparrow		
	0%	15%	30%	0%	15%	30%
CS						
Joint	97.00 \pm 0.10	82.15 \pm 3.06	73.01 \pm 4.73	-	-	-
Bare model	61.22 \pm 0.10	43.14 \pm 5.24	41.59 \pm 10.05	-45.55 \pm 0.02	-43.15 \pm 6.05	-31.36 \pm 11.32
LwF	92.51 \pm 4.10	57.48 \pm 5.07	62.28 \pm 6.75	-5.49 \pm 4.78	-30.89 \pm 6.60	-4.27 \pm 7.36
ERGNN	94.40 \pm 0.14	61.32 \pm 3.09	60.26 \pm 3.97	-3.26 \pm 0.29	-29.69 \pm 8.80	-15.50 \pm 2.88
DSLr	96.47\pm0.80	81.85\pm1.56	65.78 \pm 2.70	-2.01\pm0.88	-6.70\pm2.16	-5.04 \pm 4.40
DMSG	93.87 \pm 1.14	68.28 \pm 1.72	74.68\pm3.88	-4.24 \pm 1.43	-15.91 \pm 4.15	4.32\pm8.61
SCE	78.90 \pm 7.20	48.26 \pm 14.97	54.99 \pm 8.05	-22.48 \pm 8.69	-52.39 \pm 9.29	-27.48 \pm 17.28
CLNode	93.84 \pm 0.32	49.72 \pm 1.92	48.17 \pm 1.45	-3.84 \pm 0.47	-57.87 \pm 2.50	-58.73 \pm 1.96
TSS	79.62 \pm 5.16	48.28 \pm 4.03	49.41 \pm 12.24	-14.29 \pm 8.06	-47.73 \pm 2.55	-31.95 \pm 11.31
TFR	94.11 \pm 1.98	39.92 \pm 10.13	42.09 \pm 3.92	-3.43 \pm 2.58	-50.30 \pm 11.79	-38.35 \pm 8.88
UFO	97.29\pm0.29	91.33\pm0.32	77.70\pm1.83	-1.30\pm0.27	0.81\pm0.31	-0.84\pm1.79

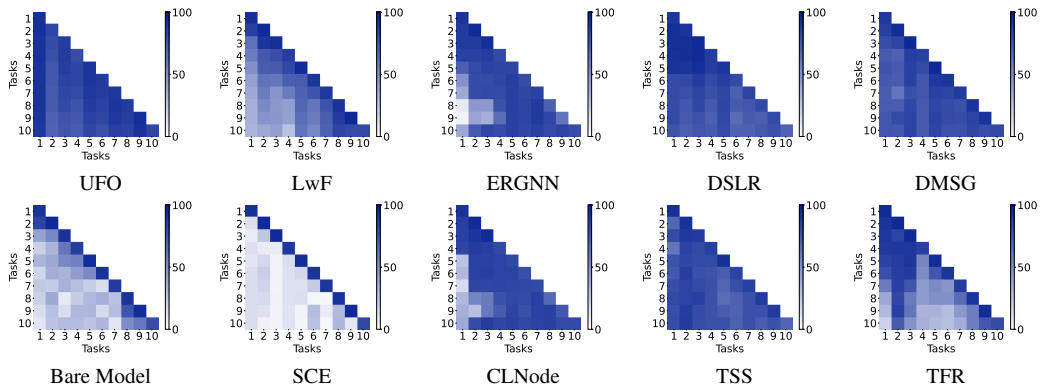


Figure 5: Performance matrices of various methods on CoraFull with 0% noise.

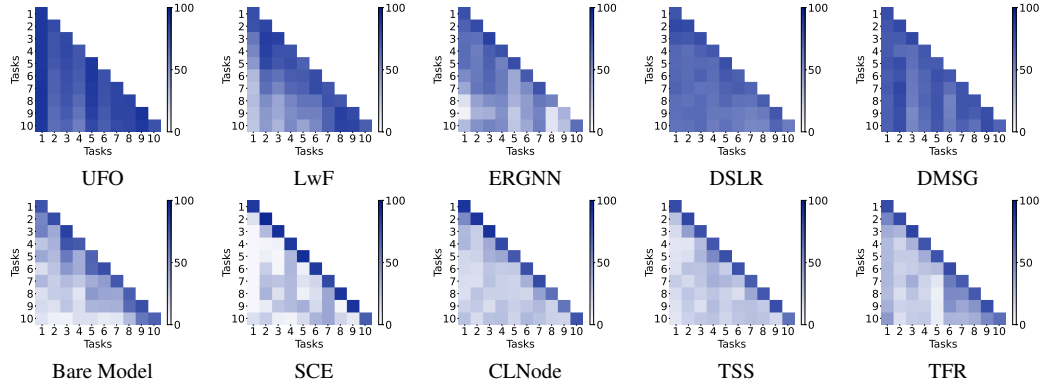


Figure 6: Performance matrices of various methods on CoraFull with 15% noise.

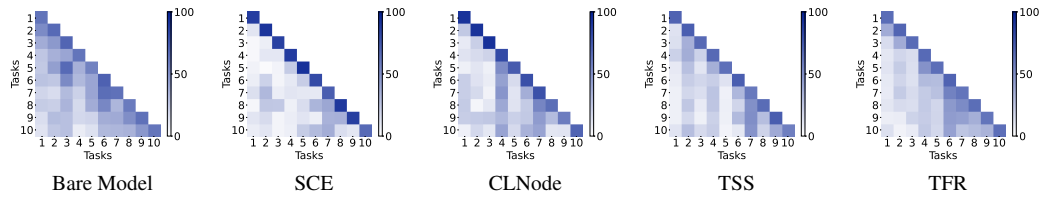


Figure 7: Performance matrices of various methods on CoraFull with 30% noise.

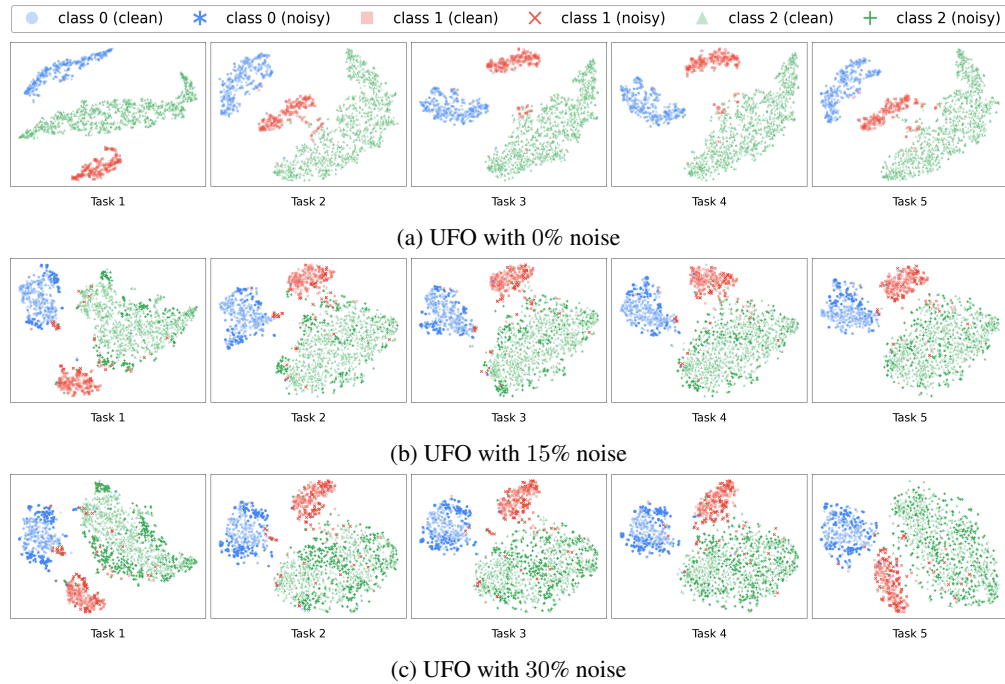


Figure 8: t-SNE visualization of the evolution of embeddings for classes 0, 1, and 2 on sequential CS.

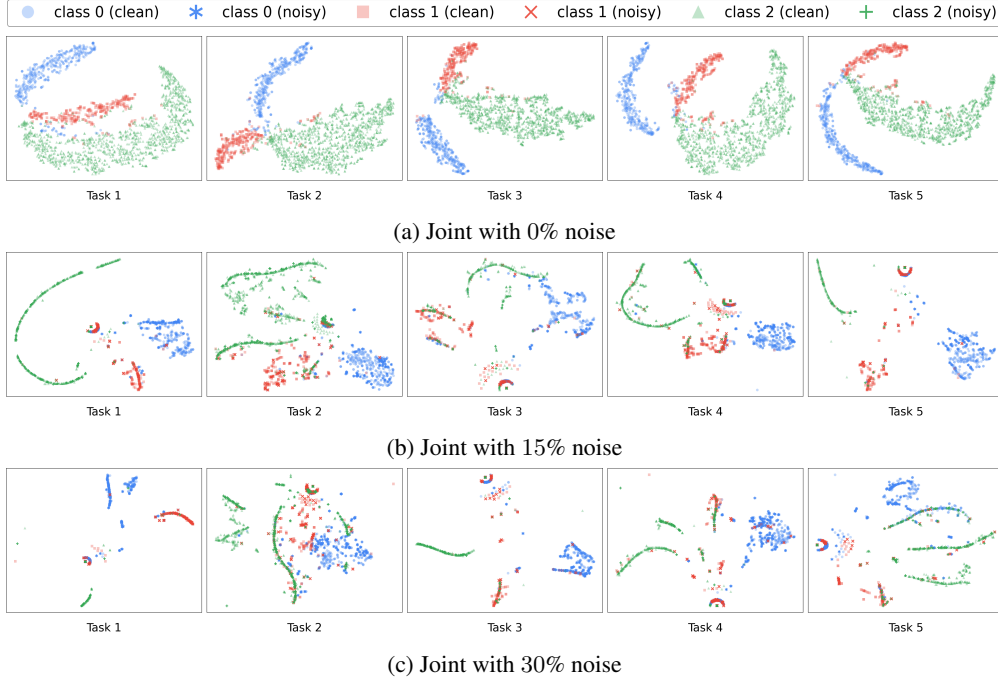


Figure 9: t-SNE visualization of the evolution of embeddings for classes 0, 1, and 2 on sequential CS.

B Additional Experimental Results

B.1 Pair Flipping Noise

In many scenarios, noisy labels are not randomly assigned to any class, but are more likely to be confused with very similar classes. For example, in the CS dataset [40], authors in paired research fields, such as machine learning and data mining or robotics and computer vision, may share similar research topics. To simulate this, we further conduct experiments under pair flipping noise with ratios of 0%, 15%, and 30%. The results are reported in Table 4, and it can be observed that UFO remains effective in preserving performance under structured label corruption.

B.2 Performance Matrices

Figures 5–7 present additional performance matrices on CoraFull under different noise ratios. As can be seen, most baselines show clear degradation on earlier tasks as the task sequence progresses, and this degradation becomes more evident when the noise ratio increases. Although some methods, such as SCE, CLNode, TSS, and TFR, produce darker diagonal regions, the lighter lower-left regions indicate limited preservation of previous task knowledge under noisy supervision. This suggests that improving robustness to noisy labels alone is not sufficient for robust continual graph learning, which further supports the need for a unified framework such as UFO to handle knowledge preservation and noisy supervision.

B.3 t-SNE Visualizations

Figures 8 and 9 show the complete visualizations of UFO and Joint on sequential CS. As can be seen, UFO maintains more compact and stable class clusters as the task sequence progresses, even when the noise ratio increases. Noisy nodes are mainly distributed near the cluster boundaries or outer regions, indicating that UFO can reduce their disturbance to the main class structure. In contrast, Joint shows more scattered embeddings under noisy supervision, especially at higher noise ratios, where the class structures become less clear. These visualizations further demonstrate the effectiveness of UFO.